

Long-range, high-resolution stratigraphic correlation of Rotliegend fluvial-fan deposits in the central Dutch offshore

De Jong, M. G.G.; Donselaar, M. E.; Boerboom, H. T.W.; Van Toorenenburg, K. A.; Weltje, G. J.; Van Borren, L.

DOI

[10.1016/j.marpetgeo.2020.104482](https://doi.org/10.1016/j.marpetgeo.2020.104482)

Publication date

2020

Document Version

Final published version

Published in

Marine and Petroleum Geology

Citation (APA)

De Jong, M. G. G., Donselaar, M. E., Boerboom, H. T. W., Van Toorenenburg, K. A., Weltje, G. J., & Van Borren, L. (2020). Long-range, high-resolution stratigraphic correlation of Rotliegend fluvial-fan deposits in the central Dutch offshore. *Marine and Petroleum Geology*, 119, Article 104482. <https://doi.org/10.1016/j.marpetgeo.2020.104482>

Important note

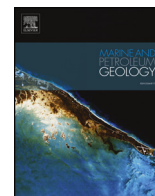
To cite this publication, please use the final published version (if applicable). Please check the document version above.

Copyright

Other than for strictly personal use, it is not permitted to download, forward or distribute the text or part of it, without the consent of the author(s) and/or copyright holder(s), unless the work is under an open content license such as Creative Commons.

Takedown policy

Please contact us and provide details if you believe this document breaches copyrights. We will remove access to the work immediately and investigate your claim.



Research paper

Long-range, high-resolution stratigraphic correlation of Rotliegend fluvial-fan deposits in the central Dutch offshore

M.G.G. De Jong^{a,*}, M.E. Donselaar^{b,c}, H.T.W. Boerboom^b, K.A. Van Toorenburg^b, G.J. Weltje^c, L. Van Borren^a^a Neptune Energy Netherlands B.V., Einsteinlaan 10, 2719 EP, Zoetermeer, the Netherlands^b Department of Geoscience and Engineering, Delft University of Technology, 2628 CN, Delft, the Netherlands^c Department of Earth and Environmental Sciences, KU Leuven, Celestijnenlaan 200E, 3001, Leuven-Heverlee, Belgium

ARTICLE INFO

Keywords:

Endorheic basin
GR pattern matching
Spectral trend analysis
Flooding surfaces
Lateral facies changes
Amalgamated alluvial ridges

ABSTRACT

The Rotliegend feather-edge area in the central part of the endorheic Southern Permian Basin in the Dutch offshore is characterized by a predominance of mud-prone, evaporite-bearing playa and lake deposits with a subordinate amount of interbedded, thin, fluvial sheet sandstones. The distribution and lateral facies changes of the sandstone bodies have been analyzed by generating a long-range, high-resolution chronostratigraphic correlation framework. The correlation technique of pattern matching of GR logs was applied, supported by calculating spectral trend curves. Flooding events are the primary near-synchronous correlation surfaces, which can be traced up to and over 100 km. The basin setting of the Southern Permian Basin, the studied sandstone depositional architecture (logs) and sedimentary characteristics (core) are analogous to the depositional setting of laterally-amalgamated terminal lobes of dryland-river systems in an endorheic basin, such as the Holocene Altiplano Basin in Bolivia, present-day Lake Eyre (Australia) and the Miocene Ebro Basin (Spain). The integrated approach has yielded a stratigraphic reservoir-architecture framework in which the reservoir sandstones, with net sand up to 10 m, have been identified as amalgamated terminal-splay sandstone sheets formed at the end of dryland-river pathways, alternating with lacustrine mudstone layers deposited during short-duration, high-magnitude flooding in intermittent wet climate periods.

1. Introduction

Permian Rotliegend aeolian and fluvial sandstones are prolific gas reservoirs throughout the Southern Permian Basin (SPB), and comprise, among others, the giant Groningen Gas Field with $2900 \times 10^9 \text{ m}^3$ GIIP (Grötsch and Gaupp, 2011). The geology, paleogeography and reservoir potential of the Rotliegend rocks in the sand-dominated southern flank of the SPB have been the subject of extensive research (Van Adrichem Boogaert, 1976; Fryberger et al., 2011; George and Berry, 1994, 1997; Verdier, 1996; Glennie, 1998; Glennie and Provan, 1990; Van Wees et al., 2000; Maynard and Gibson, 2001; Geluk, 2005, 2007; Doornbal and Stevenson, 2010; Grötsch and Gaupp, 2011; Henares et al., 2014). The overall production decline in the mature NW European Gas Province triggered the search for reservoir targets within and beyond the limits of the fairway, in part through infrastructure-led exploration. One of the target areas is the Rotliegend feather edge in the central part of the SPB in the Dutch offshore, i.e. the area where the south-derived fluvial sandstones grade to evaporite-bearing lake

deposits in the north at the interface between the Slochteren and Silverpit formations (Figs. 1 and 2). The area was to date considered marginally prospective, and the stratigraphy is characterized by a low net-to-gross, mud-prone and evaporite-bearing succession where individual sandstone sheets are below seismic resolution, and with thicknesses as low as 15 cm even below the resolution of conventional well-logging tools.

The objective of the present study is to assess the reservoir potential of thinly bedded sandstones in the mud-prone Rotliegend feather edge in the central part of the Dutch offshore (D, E, F, K and L blocks; Fig. 1). For this, a long-range (> 100 km correlation length), high-resolution stratigraphic reservoir-architecture framework is constructed applying conventional wireline-log-based well-to-well correlation which is supported by maximum-entropy spectral trend analysis of gamma-ray (GR) logs. Premises of the viability of long-range correlation are that, by analogy with the dryland-river systems in the semi-arid climate setting of the Altiplano Basin (late Quaternary, Bolivia): (1) basin-wide, correlative lacustrine mud layers formed in short-duration, high-

* Corresponding author.

E-mail address: mat.dejong@neptuneenergy.com (M.G.G. De Jong).<https://doi.org/10.1016/j.marpetgeo.2020.104482>

Received 23 December 2019; Received in revised form 19 May 2020; Accepted 20 May 2020

Available online 26 May 2020

0264-8172/ © 2020 Elsevier Ltd. All rights reserved.

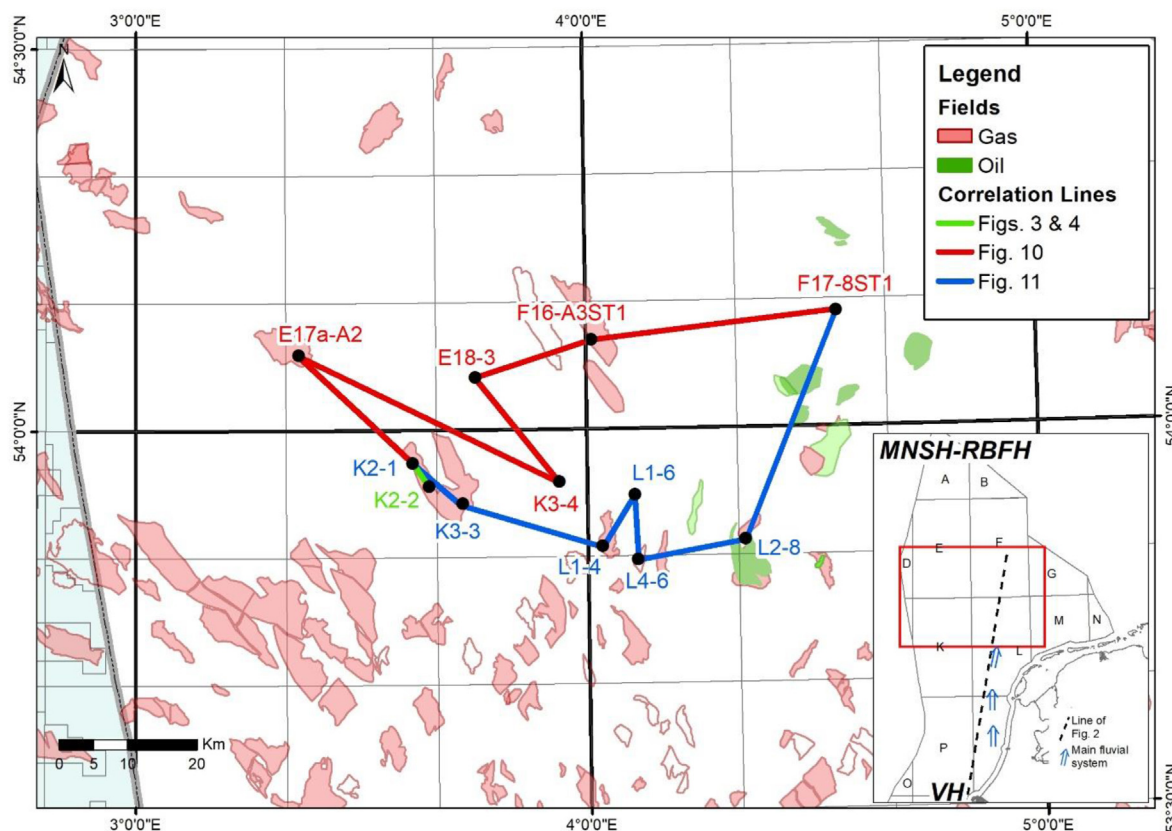


Fig. 1. Location map with wells and correlation lines presented in this paper. Blue arrows in the inset: position of the major fluvial supply system. Dashed line: position of the cross section of Fig. 2. MNSH-RBFH = Mid-North Sea High - Ringkøbing-Fyn High; VH = Variscan Highlands. (For interpretation of the references to colour in this figure legend, the reader is referred to the Web version of this article.)

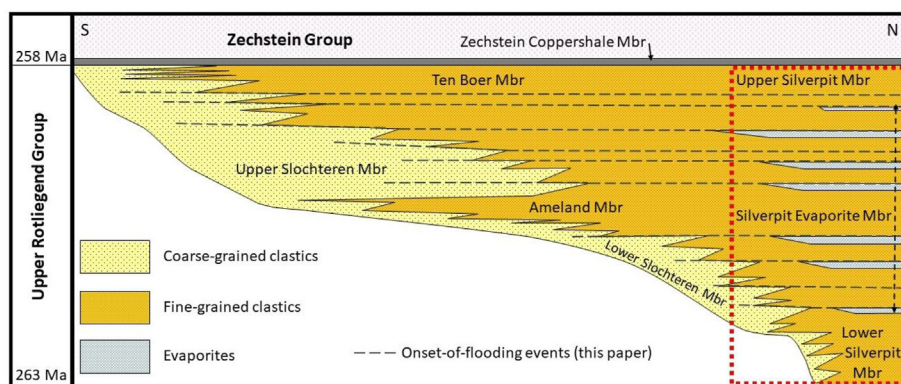


Fig. 2. Chrono-lithostratigraphy of the Dutch Rotliegend. The position of onset-of-flooding events is shown in the relation to the generalized lithofacies distribution of the members of the Slochteren and Silverpit formations. See the inset of Fig. 1 for location. Red box: stratigraphic interval and part of the basin covered in this study. Modified from: Van Adrichem Boogaert and Kouwe (1993) and Henares et al. (2014). (For interpretation of the references to colour in this figure legend, the reader is referred to the Web version of this article.)

magnitude flooding of the dryland-river coastal plain in wet climate periods (140 m base level rise and fall in only 10 ka; Baker et al., 2001; Donselaar et al., 2013,2017), and (2) laterally extensive, amalgamated sheet deposits formed at the end of the dryland-river path by compensational stacking of terminal-splay sediments (Fisher et al., 2007, 2008; Donselaar et al., 2013; Van Toorenburg, 2018; Van Toorenburg et al., 2018).

Dryland river systems have been studied among others in the Ebro Basin (Tertiary, Spain) and Lake Eyre (late Quaternary, Australia) (Fisher et al., 2007, 2008; McKie, 2011; Sáez et al., 2007), thus offering potential analogues for the Rotliegend. The Altiplano Basin is the primary analogue of depositional processes in this study, because both lowstands and highstands are well documented, thus offering a modern full-cycle analogue for the Rotliegend.

2. Geological setting

The Rotliegend sediments in The Netherlands are part of the Lower Permian Upper Rotliegend Group (URG) (Van Adrichem Boogaert and Kouwe, 1993). The URG sediments accumulated in the large west-east trending SPB, which extended from eastern England to Poland and was bounded to the south by Variscan Highlands (London-Brabant and Rhenish Massifs) and to the north by the Mid-North Sea High and the Ringkøbing-Fyn High (Fig. 1). In a setting of tectonic quiescence after the Variscan Orogeny, subsidence of the SPB is attributed to thermal contraction of the lithosphere (Van Wees et al., 2000), thus allowing application of the concepts of layer-cake stratigraphy and ramp-like facies-belt transitions. The SPB was an endorheic basin (Glennie, 1998; De Jager, 2007; Van den Belt and Van Hulten, 2011). Core and well-log analyses from the German part of the URG (Legler and Schneider, 2008) suggest rare intermittent connection with the marine environment of

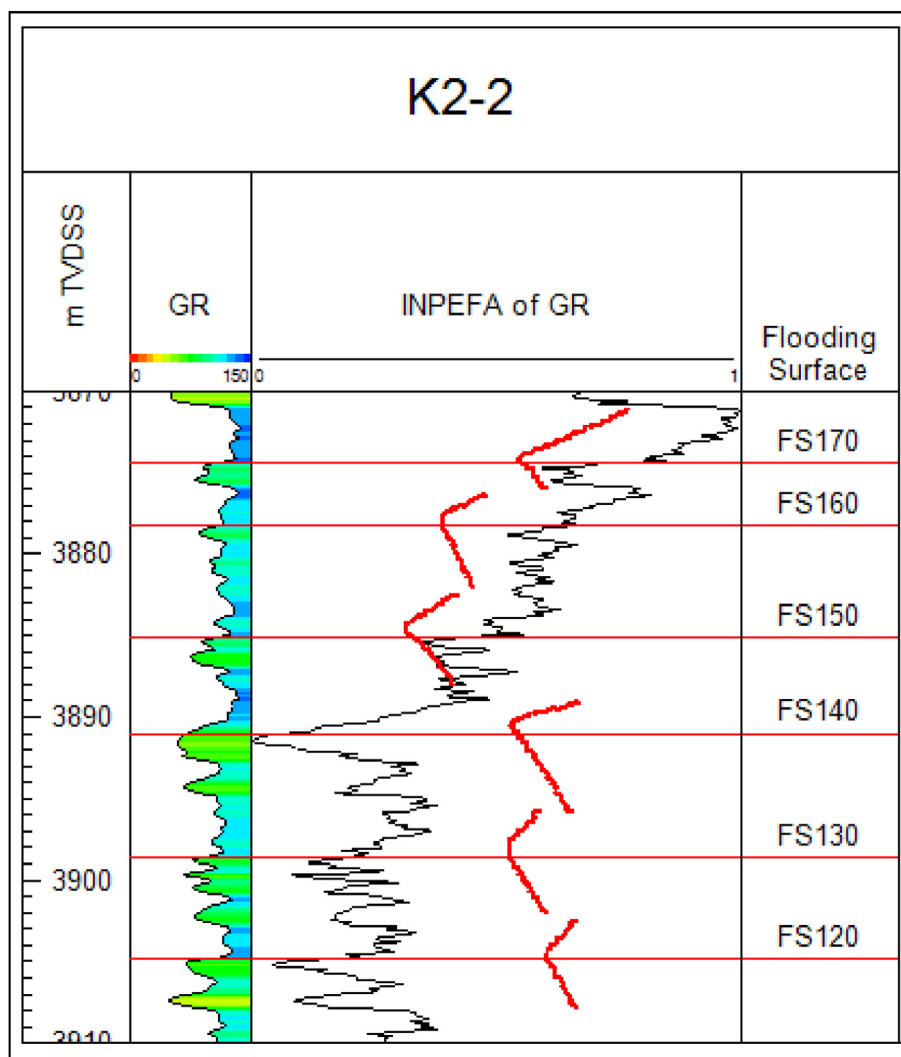


Fig. 3. Short section of the Rotliegend in well K2-2. See Fig. 1 for location. Key to vertical tracks: 1 - Depth (m TVDSS); 2 - GR (natural gamma-ray log, API scale; colouring to highlight variation in values); 3 - Spectral trend curve (INPEFA) of GR data (scale dimensionless from 0 to 1); 4 - Flooding surfaces (FS, this paper). C-shape patterns identified and correlated in this study are indicated in red in track 3. Also note the overall coarse-grained nature of the interval below FS140 and the fine-grained character above. (For interpretation of the references to colour in this figure legend, the reader is referred to the Web version of this article.)

the Arctic rift system between East Greenland and the Fennoscandian Shield; three minor short-termed incursions are reported, with influx of a limited amount of marine water only and no impact on the lithofacies succession. The SPB basin fill in the Dutch sector largely consists of continental siliciclastic and evaporite sediments formed in an arid climate setting during base-level lowstands. Extensive evaporite-bearing lake deposits occupy the basin centre (Silverpit Evaporite Member, Fig. 2), and are fringed by playa mudflats and sandflats with aeolian dune deposits (Lower and Upper Slochteren members). South-north running rivers dissected the aeolian domain (Van Adrichem Boogaert, 1976; Glennie, 1998; George and Berry, 1994; Verdier, 1996; Geluk, 2005, 2007; Donselaar et al., 2011). The fluvial sediments were sourced from the Variscan Highlands in the south and show a suite of proximal channelized conglomerates and sandstones to distal sandy unconfined sheetflood deposits (Donselaar et al., 2011). Recently some of the larger, mappable fluvial fairways cross-cutting the Rotliegend have been interpreted as fluvial fans (Fryberger et al., 2011; Moscariello, 2005, 2017).

The large-scale URG palaeogeographic setting and spatial relation of the depositional environments is captured in a lithostratigraphic framework (Van Adrichem Boogaert and Kouwe, 1993, Fig. 2). High-resolution, reservoir-scale correlation is hampered by the absence of

continuous biostratigraphic markers in the continental barren red-bed deposits and by the poor imaging of seismic data below thick Zechstein salts (Van Ojik et al., 2011). Techniques akin to or rooted in sequence stratigraphy (Catuneanu et al., 2009) are often applied nowadays, usually revolving around the concept of (maximum) flooding, wetting, or abandonment surfaces as the near-synchronous markers of wide lateral extent (George and Berry, 1994; Howell and Mountney, 1997; Maynard and Gibson, 2001; Minervini et al., 2011; Van den Belt and Van Hulst, 2011; Van Ojik et al., 2011; Dalman et al., 2015).

A high-resolution stratigraphic correlation of the thinly bedded Silverpit Formation deposits has not yet been published. Van Ojik et al. (2011) presented a large-scale lithostratigraphic framework for the claystone-dominated evaporite-bearing succession of the Silverpit Formation: Lower Silverpit Member, Silverpit Evaporite Member and Upper Silverpit Member (Fig. 2). The Upper Silverpit Member merges to the south into the claystone-dominated Ten Boer Member (Van Ojik et al., 2011). Donselaar et al. (2011) presented a stratigraphic correlation framework of the Ten Boer Member to map out the spatial distribution of thin fluvial sheet sandstones.

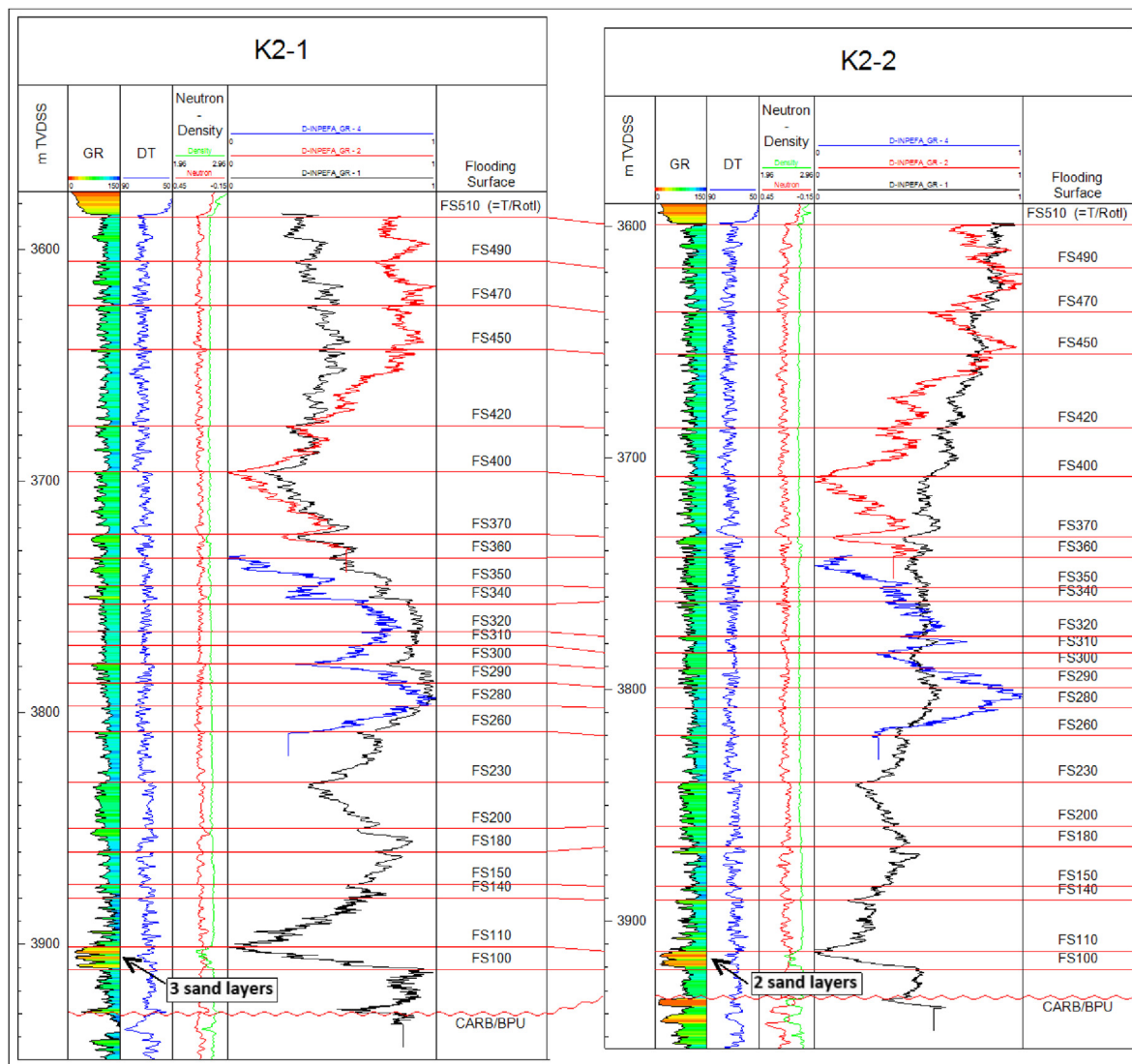


Fig. 4. Correlation diagram of the total Rotliegend interval in wells K2-1 and K2-2. See Fig. 1 for location. Key to vertical tracks: 1 - Depth (m TVDSS); 2 - GR (natural gamma-ray log, API scale; colouring to highlight variation in values); 3 - DT (sonic log, $\mu\text{sec}/\text{ft}$); 4 - Neutron and Density logs (fraction and g/cc, resp.); 5 - Spectral trend curves (INPEFA) of GR data (scale dimensionless from 0 to 1); 6 - Flooding surfaces (FS, this paper; T/Rotl = top of the Rotliegend, corresponding with the base of the Copper shale Member of Van Adrichem Boogaert and Kouwe (1993); CARB/BPU = top of Carboniferous/Base Permian Unconformity). Datum plane is FS230. (For interpretation of the references to colour in this figure legend, the reader is referred to the Web version of this article.)

3. Data and methodology

3.1. Data

Well-log data from all exploration and appraisal wells in the study area (Fig. 1) have been used for generating the high-resolution correlation framework. In addition, well logs from development wells of the gas fields in the study area have been analyzed, together amounting to more than 80 wells. The lithofacies characteristics of the sandstones, siltstones and claystones at the interface of the Silverpit Formation and the Lower Slochteren Member, in the lower part of the Rotliegend, were analyzed from 55 m of core from wells E17-3, K2-1, K2-2 and K3-1 in the K2b-A gas field. Lithofacies description followed the convention of Reijers et al. (1993).

3.2. Wireline-log correlation methodology

3.2.1. Log correlation of flooding surfaces

The correlation technique employed in this study is based on pattern matching of trends and trend changes in the lithofacies succession as

expressed in wireline logs, notably gamma-ray (GR) logs. The correlation method is a simplified version of De Jong et al. (2006, 2007), Nio et al. (2006) and Van Ojik et al. (2011) with focus on trend changes from coarser-grained to finer-grained lithologies (flooding trend) only, as opposed to the previous studies that also consider trend changes from finer-grained to coarser-grained lithologies (progradational trend). The choice is based on the concept that in endorheic basins a change from drier to wetter climate conditions results in short-duration, high-magnitude lake-level highstands, with high preservation potential in the basinal sedimentary record. The reason for this is that in an inland basin the increase of meteoric water is not dissipated in the world's oceans, but stored in the basin confinement. Kessler (1984), Bills et al. (1994), Blodgett et al. (1997), Sylvestre et al. (1996, 1999), Argollo and Mourguiart (2000), Fornari et al. (2001) and Placzek et al. (2006) described high-magnitude, short-duration lake-level rise and fall cycles in the Late Pleistocene-Holocene Altiplano Basin of Bolivia with lake level fluctuations of 55–140 m, and a total duration of 2–11 ka. The impact of climate change on the sedimentary architecture of the basin fill is that such drastic base-level changes cause rapid drowning of the low-gradient floodplain and the (saliferous) lake in the basin centre. The

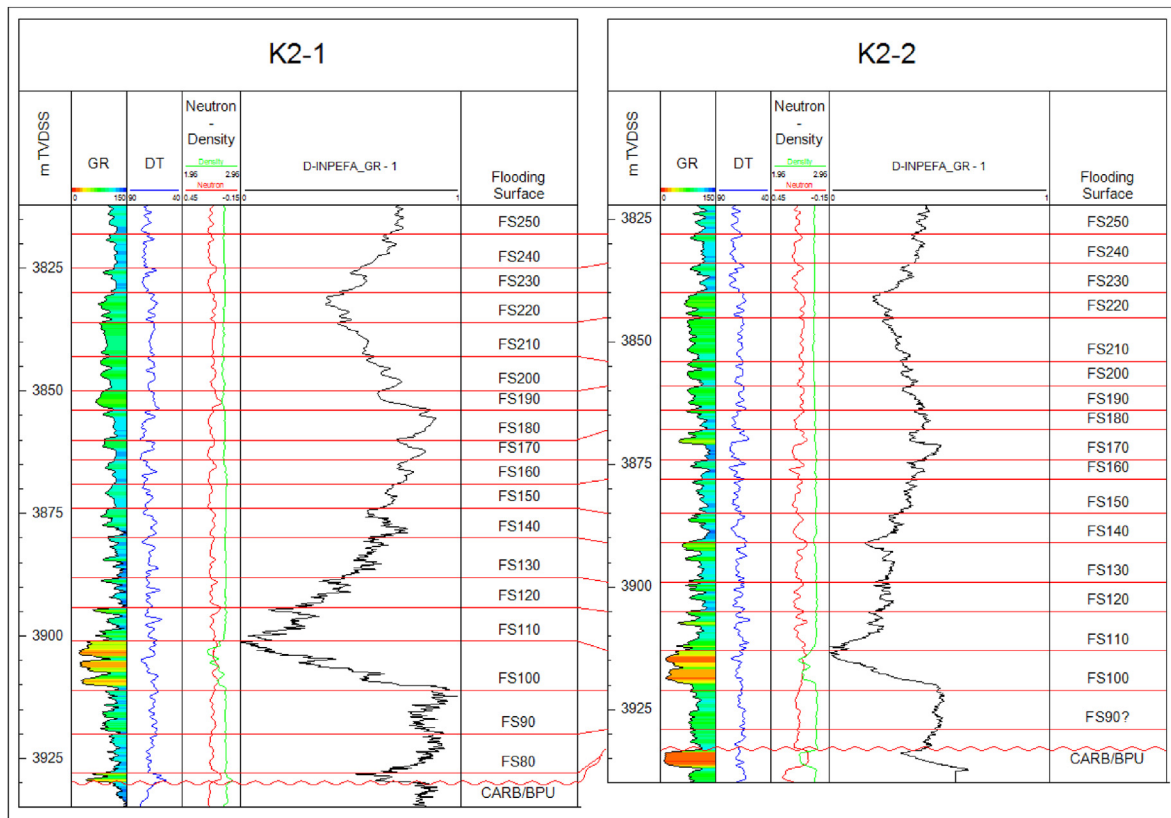


Fig. 5. Lower part of Rotliegend in wells K2-1 and K2-2 (from: De Jong et al., 2017). See Fig. 1 for location. Key to tracks as in Fig. 4. Datum plane is FS230. The low-GR beds capped by FS110 are fluvial sands; the thin low-GR layer overlying Carb/BPU in K2-1 consists of debris-flow deposits (observed in core). Three thin sand layers are present in K2-1 between FS100 and FS110, two in K2-2; the lower two layers in K2-1 are amalgamated in K2-2. (For interpretation of the references to colour in this figure legend, the reader is referred to the Web version of this article.)



Fig. 6. Low-angle climbing-ripple and wavy lamination observed in cores of well K3-1 (left: 3920 m; right: 3923 m). The structures are indicative for crevasse-splay deposits. The same structures are observed in the crevasse splays of the fan of the Río Colorado in the Altiplano Basin. (For interpretation of the references to colour in this figure legend, the reader is referred to the Web version of this article.)

erosive power associated with rapid lake-level rise in a low-gradient setting is weak, owing to the absence of wave and tides, hence reworking of the floodplain deposits is limited. An extensive, basin-wide, continuous blanket of lacustrine mud is draped over the previously deposited lowstand deposits (Donselaar et al., 2013; Van Toorenburg, 2018; Van Toorenburg et al., 2018). Such rapid, basin-wide transitions from coarser-grained fluvial deposits to finer-grained distal fluvial and lake deposits may thus be interpreted as near-synchronous flooding surfaces. The flooding surfaces and highstand deposits of the Rotliegend in the endorheic SPB are inferred to have formed under similar conditions (Donselaar et al., 2011).

Conceptually similar correlation methods, with focus on wetting surfaces, have been applied in the sandstone-dominated aeolian and fluvial section to the south of the present study area (Martin and Evans, 1988; George and Berry, 1994, 1997; Howell and Mountney, 1997; Minervini et al., 2011; Van den Belt and Van Hulst, 2011), which paves the way for extending the present correlation framework to the basin margin in the south.

3.2.2. Maximum entropy spectral trend curves

Gamma-ray (GR) log-pattern identification and well-to-well correlation was done by visual interpretation, facilitated by graphical display enhancements such as well-specific horizontal scaling and colouring. Core GR usually shows better bed definition in the fine-grained deposits than the conventional logs, highlighting the alternation of beds. In addition, GR logs were treated as composite waveforms on which time-series analysis was performed. Maximum-entropy spectral trend curves of the GR data were generated with CycloLog software as a means to graphically evaluate the validity of the visually matched patterns of the unprocessed data (Figs. 3–5). The maximum entropy spectral trend curve is the integral of the prediction errors, i.e., the differences (errors) between a data series and a linear filter optimized to predict data-points ahead of a sliding window. The spectral trend curve can also be thought of as expressing changes in the spectral content of the data; the power spectrum of the data can be calculated from the prediction filter. The curve is commonly referred to as INPEFA, an acronym for Integrated Prediction Error Filter Analysis (Nio et al., 2006; De Jong et al., 2009, 2019; Van Ojik et al., 2011; Qayyum and Smith, 2014). Key feature of

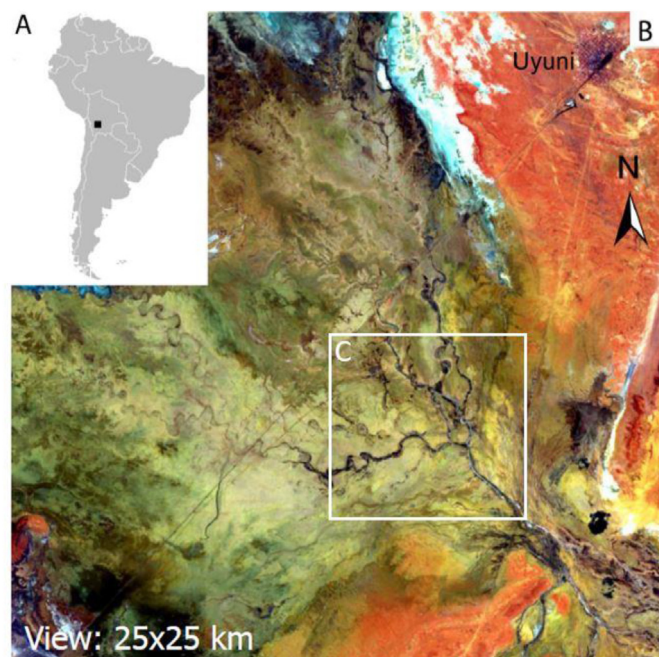


Fig. 7. A – Location of the Uyuni and Río Colorado area in Altiplano Basin of Bolivia; B – 25×25 km Landsat image of the northwest-flowing Río Colorado terminus with a branching pattern of avulsed former river paths; C – location of Fig. 8 (from: Donselaar et al., 2017). Note that the channelized part of the fan is small compared with the area of unconfined deposits (crevasse splays, basinal fines). (For interpretation of the references to colour in this figure legend, the reader is referred to the Web version of this article.)

the INPEFA curve is that it highlights trends and trend changes in the input data. Specifically, it aids in evaluation of vertical lithofacies changes in the GR log and permits inference of stacking patterns. The spectral trend curve is always normalized to values between 0 and 1 and, hence, calculating the INPEFA from part of a data set generally increases the apparent variance compared with the same segment in the curve of the complete processed data set. As a result, the patterns of the former curve are more pronounced than those of the INPEFA curve from the total data set (Qayyum and Smith, 2014), which facilitates the identification of lithofacies patterns (compare the coloured INPEFA curves with the black curves in Fig. 4). For a discussion of the pitfalls and caveats in the use of INPEFA refer to Qayyum and Smith (2014).

The matched patterns in the GR logs of the present study are essentially relatively coarse-grained or coarsening-upward bed successions, alternating with relatively fine-grained or fining-upward bed successions. The former are usually thick and locally show scour features at the base, the latter are thin. In geological terms, the base of the fining-upward bed succession represents the onset of the short-duration, high-magnitude flooding event in the endorheic basin, and therefore the flooding surface (FS) is the primary near-synchronous correlation surface. The approach to correlating bears resemblance to the genetic sequence stratigraphy of marine basin margins proposed by Galloway (1989). The packages between the flooding surfaces are the terrestrial portions of chronosomes (chronostratigraphically constrained lithosomes) as defined by Dalman et al. (2015). This approach facilitated the evaluation of lateral and vertical facies changes within the framework of near-synchronous boundaries.

The envelope of a coarser-grained interval overlain by a finer-grained interval resembles a C-shape in the GR and INPEFA curves, with a typical thickness of 5–10 m (Fig. 3). The correlated surfaces in the GR curve correspond with “up-to-the-right” turning points in the INPEFA curves, while the coarser-grained bed successions correspond with “up-to-the-left” trends in the INPEFA curves and the finer-grained bed successions with “up-to-the-right” trends.

Fig. 4 illustrates the surfaces used for the correlations and the correlation for the total Rotliegend interval in the closely spaced wells K2-1 and K2-2 in the K2b-A gas field, whereas Fig. 5 zooms in on the lower part of the section and therefore shows a higher density of correlated surfaces. The overall similarity of patterns between the wells is high, both in the GR curves and in the corresponding spectral trend curves, pointing to an overall tabular geometry of units in the area. It is important to realize that relative lithofacies patterns, i.e. trend and trend changes of lithologies, are matched between wells, and not lithologies as such; the matched patterns in the GR and trend curves are not identical, they are similar or equivalent. Note that the change from finer-grained (bottom) to coarser-grained (top) packages is less distinct, gradational, in many cases; for reasons of legibility these boundaries are not displayed in Figs. 3, 4 and 5. The sections of Figs. 3, 4 and 5 suggest a hierarchical stratigraphic architecture in some intervals: correlated C-shapes or flooding surfaces are superimposed on larger-scale patterns. For instance, FS140 in Fig. 3 is the boundary between an underlying overall coarse-grained section and an overlying overall fine-grained section. Other examples are at FS230 and FS370 in Figs. 4 and 5. Over short distances, or on field scales, such patterns often show some degree of lateral persistency, and facilitate making high-resolution correlations. These larger scale trends are often not persistent on a regional scale, due to overall lateral changes in sediment calibre. High-resolution correlating, however, is not affected. Bearing in mind that our focus is on details, the stratigraphic scheme of flooding surfaces here presented, therefore, is non-hierarchical.

4. Results

4.1. Lithofacies associations and depositional setting

A wealth of core descriptions is available for the Rotliegend in the Dutch offshore. The core atlas of Mijnlief et al. (2011) is a thorough compilation and reference handbook. Here, a brief description is presented of the lithofacies observed in the cores from wells E17-3, K2-1, K2-2 and K3-1, which are representative for the main clastic facies in the central Dutch offshore. The cores consist predominantly of an intercalation of claystone and siltstone and very fine-grained to fine-grained sandstone deposits. Four lithofacies types were described on the combination of sandstone to claystone-siltstone ratio, dominant sedimentary structures and bed thickness: (1) Playa mudflat and lake deposits, dominantly consisting of thin-bedded to massive claystone to siltstone, (2) Terminal-splay deposits, made up of interbedded thin siltstones to sandstones, (3) Fluvial-channel deposits, comprising thick-bedded sandstones, and (4) aeolian dune deposits.

4.1.1. Lithofacies association 1 - playa mudflat and lake

This lithofacies association comprises structureless and massive, up to 5-m-thick red-brown claystone intervals, and thin, interbedded (individual bed thickness 0.2–3 cm), red-brown claystone to brown-grey coarse siltstone. The base of the beds is sharp to gradational. The top is generally sharp. Parallel lamination is the dominant sedimentary structure; wavy lamination and low-angle climbing-ripple lamination are common (Fig. 6). Sand dykes and synaeresis cracks occur occasionally. Soft-sediment deformation is present in the form of flame-, slump- and seepage structures. Small anhydride grains are observed.

4.1.2. Lithofacies association 2 - terminal splays

The facies consists of red-brown, thin-bedded, very-fine to medium-grained sandstone and siltstones. Individual beds are 10–40 cm thick and may stack up to 1 m. When stacked, mudstone may be present between the sandstone beds. Lower bed boundaries are sharp and scoured, the upper boundaries are in general gradational. Individual beds may fine upward to claystone. Granule stringers are occasionally observed. Sedimentary structures include wavy lamination, parallel lamination and low-angle climbing-ripple lamination. Water-escape

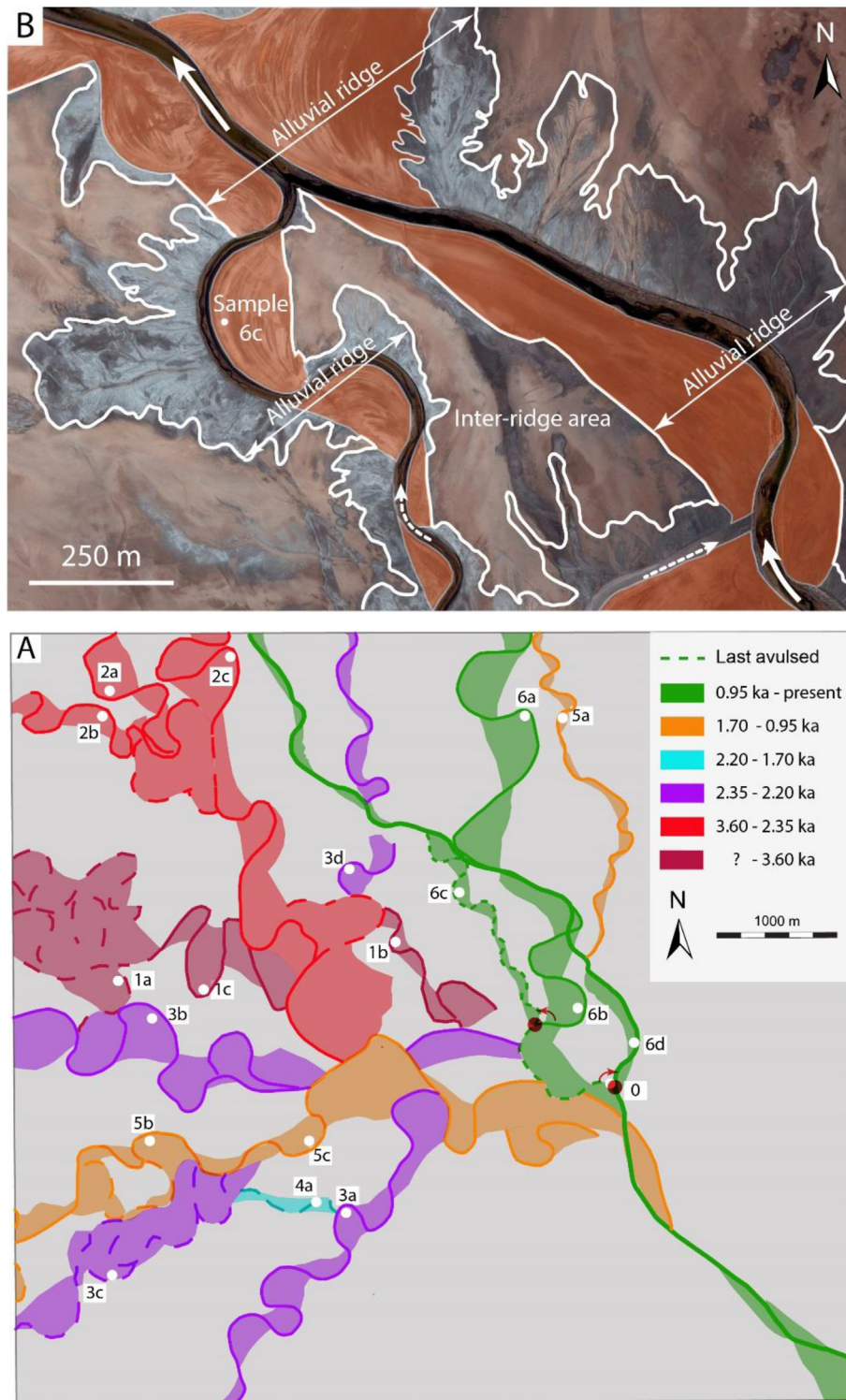


Fig. 8. A - Río Colorado avulsed channel-belt network (from: [Donselaar et al., 2017](#)). B - Formation of alluvial ridges by the lateral expansion and vertical aggradation of point bars (brown) and crevasse plays (outlined). Present-day river flows to the northwest (solid line with arrow). Last-avulsed river: dashed line plus arrow. (For interpretation of the references to colour in this figure legend, the reader is referred to the Web version of this article.)

structures are common. Bioturbation can be observed in the form of rootlets. The red-brown coloured beds have whitish cement spots throughout the facies.

4.1.3. Lithofacies association 3 - fluvial channels

The brown-ocre coloured sandstone beds of the facies are up to 1.75 m each. The facies forms stacks of up to 2.5 m in thickness where

generally no claystone is present between the separate beds. The top is gradational to sharp. The base is sometimes scoured. The grain size ranges from very fine to medium sand. No indicative trend can be identified. Large-scale trough cross bedding is present and forms the main sedimentary structure of the facies. Individual sets are up to 50 cm in thickness. Parallel lamination can also often be observed, sometimes combined with a bimodal grain-size distribution. Occasional clay

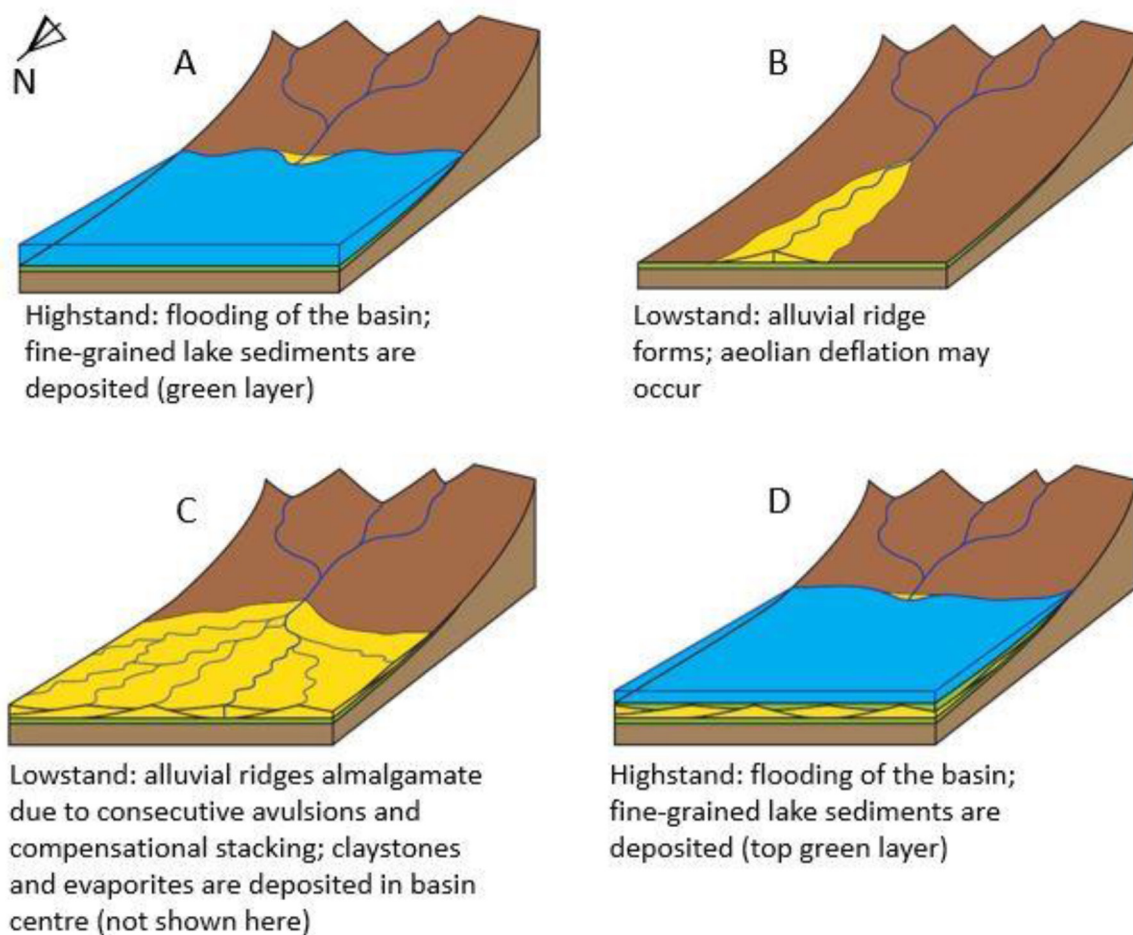


Fig. 9. Schematic representation of the formation of alternating coarser-grained highstand and finer-grained lowstand deposits as a function of base-level changes: from A to B to C to D. A – highstand period, a thin layer of fine-grained lake deposits (green layer) forms. B – lowstand period, the fluvial system starts to build out into the basin, channels and crevasse splays form an alluvial ridge (downstream floodbasin & playa deposits and evaporites not shown). C – lowstand period, alluvial ridges amalgamate due to consecutive avulsions and compensational stacking. D – highstand period, fine-grained lake deposits (green layer) form (as in A). (For interpretation of the references to colour in this figure legend, the reader is referred to the Web version of this article.)

drapes can be identified within the unit. Granule stringers and anhydride grains are sometimes present. Cementation gives the layers often a white bloom.

4.1.4. Lithofacies association 4 - aeolian dunes

This lithofacies comprises cross-laminated sandstone with a typical bimodal medium-coarse and very-fine-fine grain-size distribution. It occurs as occasional, subordinate intercalations in Lithofacies association 3. Beds are thin (decimeter-scale) with erosional tops. Internally the laminae are moderately- to well-sorted. It may have formed as aeolian dunes, produced by the grain-flow and grain-fall depositional process.

4.1.5. Depositional setting

The claystone and siltstone deposits (Lithofacies association 1) formed in a wet playa mudflat environment, largely under evaporitic conditions. The red-brown and brown-grey colours suggest alternating drier and wetter conditions, the latter including lacustrine conditions. The thin-bedded sandstones and siltstones (Lithofacies association 2) formed by incursions of unconfined terminal splays into the playa mudflat. Sedimentary structures such as the sharp and scouring lower bed boundaries, climbing-ripple and parallel lamination are characteristic for high-energy sheet flows, and the normal grain-size grading, wavy lamination, and rootlet bioturbation point to waning flow conditions and subsequent vegetation. Similar sedimentary

characteristics have been described extensively from terminal-splay deposits in alluvial ridges in a modern-day analogue setting at the edge of the Salar de Uyuni (Altiplano Basin, Bolivia; Fig. 7; Donselaar et al., 2013; Van Toorenburg, 2018; Van Toorenburg et al., 2018). The thicker-bedded, slightly coarser-grained sandstones (Lithofacies association 3) are interpreted as the upstream river-channel deposits that connect to the terminal-splay deposits. Donselaar et al. (2013) and Van Toorenburg (2018) documented extensive, laterally-amalgamated sand sheets with a correlation length of 25 km at the terminus of the present-day Río Colorado (Altiplano Basin, Bolivia) deposited by compensational stacking of terminal-splay sands after multiple upstream river avulsions, and overlying a very-low gradient exposed lacustrine topography which facilitated uninhibited, long-range lateral switching of the river system (Fig. 8). The lateral and vertical facies variations in the sandy lowstand deposits of the Rotliegend of the Rotliegend in terms of such laterally-amalgamated sand sheets. Noteworthy is that crevasse splays are volumetrically the most important deposits of the Río Colorado fan (Fig. 7). The aeolian dune deposits are most likely wind-reworked sands from Lithofacies associations 2 and 3. Their preservation potential in the predominantly fluvial environment is low. Conversely, Lithofacies association 4 is sometimes interpreted as fluvially reworked aeolian dune material.

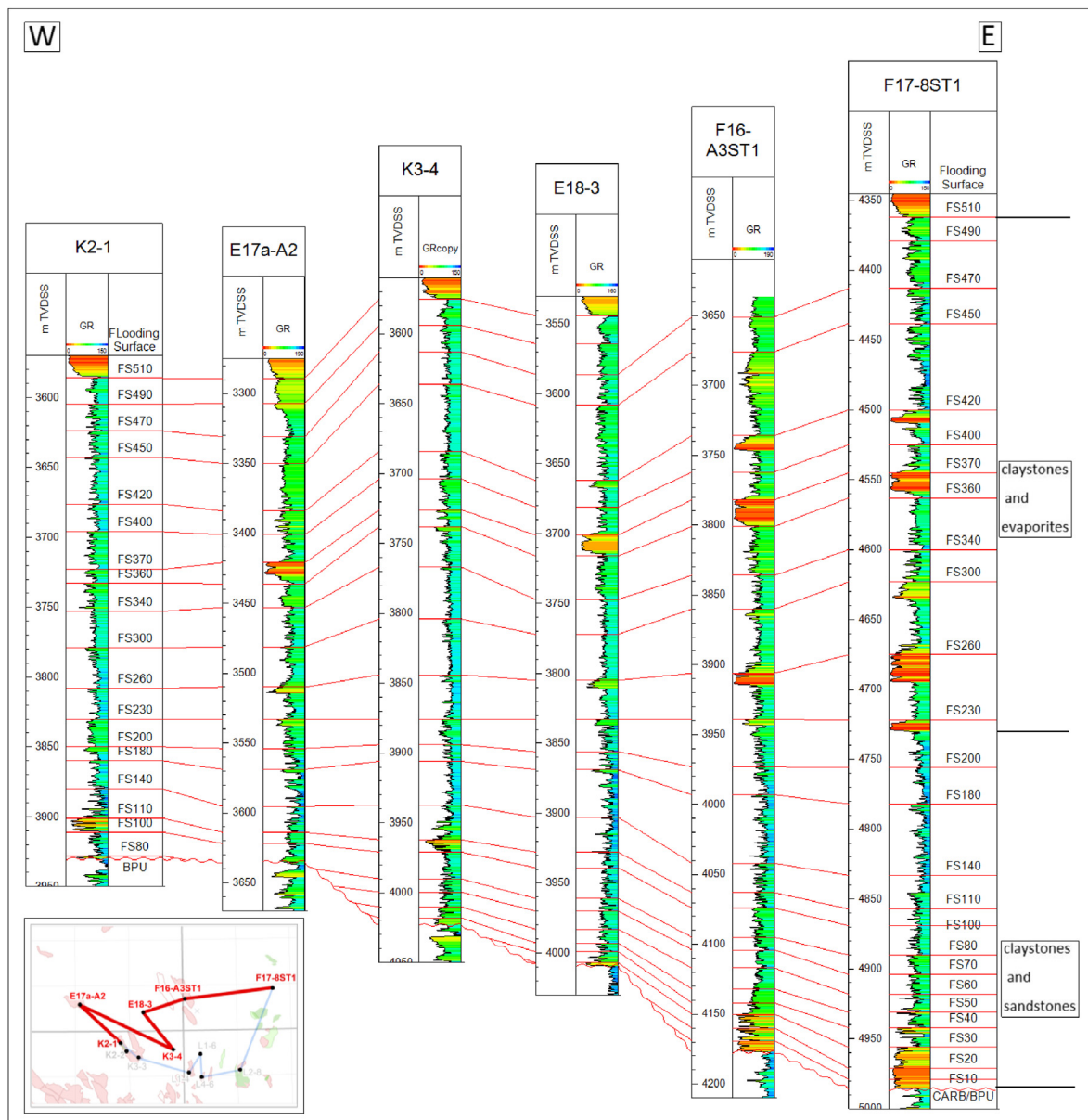


Fig. 10. Regional well-to-well correlation diagram from K2-1 to F17-8ST1 along a northern transect through the feather-edge area (from: De Jong et al., 2017). See also Fig. 1 for location. Key to vertical tracks: 1 - Depth (m TVDSS); 2 - GR (natural gamma-ray log, API scale; colouring to highlight variation in values); 3 - Flooding surfaces (FS, this paper; FS510 = top of the Rotliegend, corresponding with the base of the Coppershale Member of Van Adrichem Boogaert and Kouwe (1993); CARB/BPU = top of Carboniferous/Base Permian Unconformity). Datum plane is FS230. The low-GR beds above FS200 are evaporite layers, while the low-GR beds below FS200 in all wells consist of clastics. Not all identified and correlated flooding surfaces are displayed, for reasons of legibility. (For interpretation of the references to colour in this figure legend, the reader is referred to the Web version of this article.)

4.2. Regional correlation framework and basin fill

Generating the well-to-well correlation framework and stratigraphic scheme started in the K2b-A Field (Figs. 1, 3–5). The close spacing the large number of wells enabled the identification of flooding surfaces with good inter-well reproducibility, and facilitated the assessment of lateral facies variations within the framework of near-synchronous flooding surfaces (Figs. 6–8). In a subsequent step, the high-resolution stratigraphic framework of the K2b-A Field was expanded step-by-step and as much as possible in loop-ties of wells in all directions to cover the southern D, E and F blocks and the northern K and L blocks (Fig. 1). The flooding surfaces are markers of wide lateral extent, and the packages bounded by the surfaces are sheet-like. As in K2b-A, the coarser-grained units are usually thicker than the finer-grained units. In terms of depositional processes, a low-gradient fluvial distributary

system – a very large fluvial fan – expanded and contracted in a regular fashion, controlled by basin-scale fluctuations in base level, producing a stacking of relatively coarse-grained lowstand deposits alternating with relatively fine-grained highstand deposits in a subsiding basin (Figs. 9–11). The observed morphology and the dimensions of the amalgamated alluvial ridges of the Río Colorado fit with the wireline-log-derived stratigraphic architecture of stacked tabular sheet-like deposits of the URG.

The high-resolution framework of flooding surfaces in combination with the fluvial-fan depositional model enables the evaluation of lateral facies changes, including the distribution of thin potential reservoir sands, as illustrated by the following example. The sandstones of the K2b-A Field, i.e. the sandstones capped by FS110, are also present in the wells of the K and L blocks, while they grade to relatively fine-grained sediments in the wells of the E and F blocks (Figs. 10 and 11). The facies

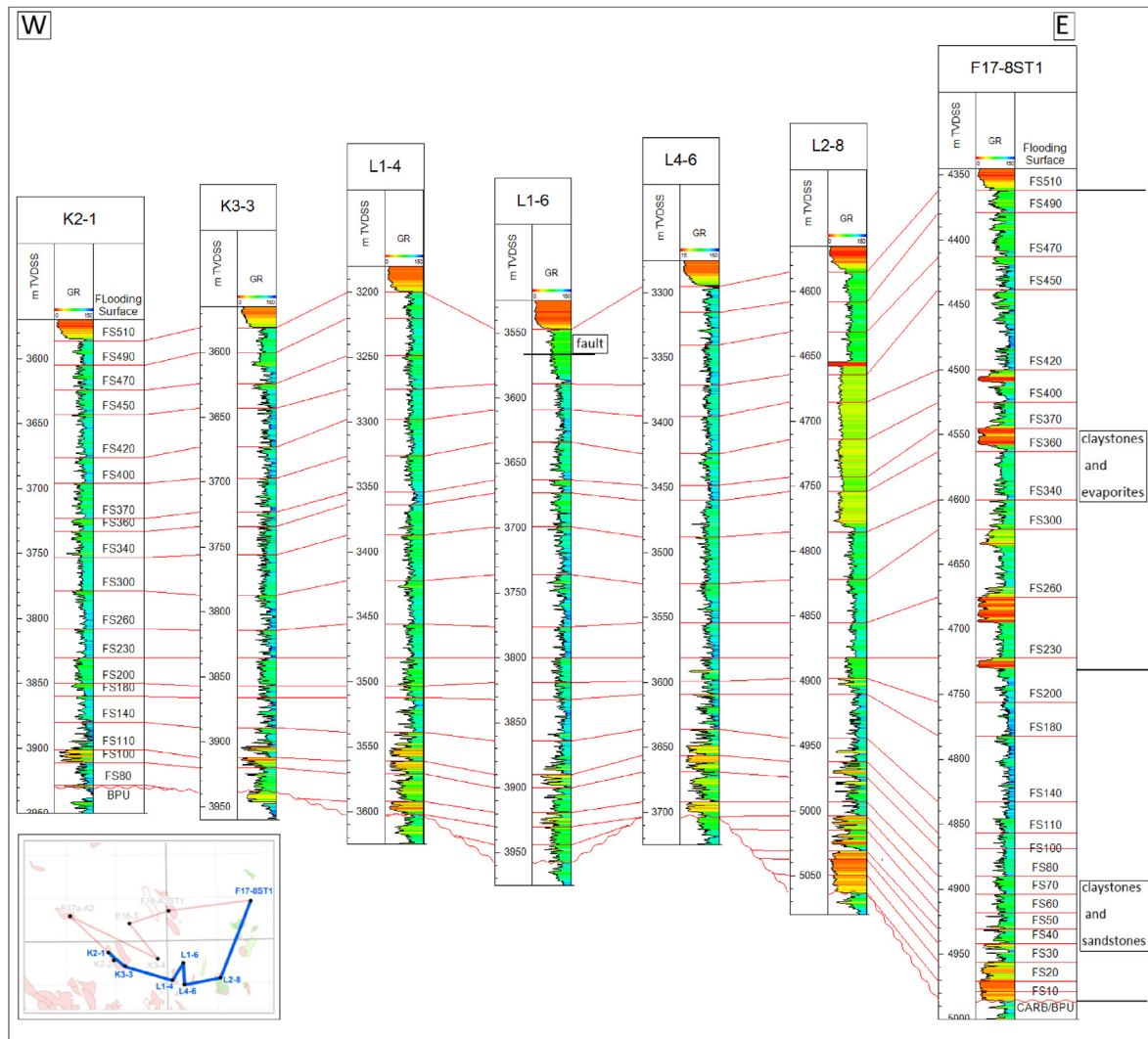


Fig. 11. Regional well-to-well correlation diagram from K2-1 to F17-8ST1 along a southern transect through the feather-edge area. See also Fig. 1 for location. Key to tracks as in Fig. 10. Datum plane is FS230. The low-GR beds above FS200 are evaporite layers, while the low-GR beds below FS200 in all wells consist of clastics. Well L1-6 is interpreted to have drilled through a fault, causing a reduced uppermost section. Not all identified and correlated flooding surfaces are displayed, for reasons of legibility. (For interpretation of the references to colour in this figure legend, the reader is referred to the Web version of this article.)

distribution of the package between FS110 and FS140 shows a similar pattern, with one notable exception: sands have graded to fines in wells K2-1 and K2-2 (Fig. 5). The post-FS140 section is essentially sandstarved. The conclusion is that the study area became progressively more distal, consistent with the overall back-stepping of the fluvial-fan depositional system from the basin centre towards the southern basin margin (e.g. Van Ojik et al., 2011, Fig. 2).

The correlations of Figs. 10 and 11 show the oldest deposits to occur in wells F16-A3ST1, F17-8ST1 and L2-8. The basal, pre-FS30, sands in L2-8 and in the L5 block to the south (not shown here) are amalgamated and are interpreted as confined channel deposits. A stratigraphic subdivision of this package is not easily made, given that relatively fine-grained intercalations – i.e. potential transgressive/highstand deposits – are lacking. Note that the preservation potential of the latter is low in the confined environment owing to repeated reworking and bypassing. Equivalent pre-FS30 deposits occur in F16-A3ST1 and F17-8ST1, with a clear alternation of finer-grained and coarser-grained deposits. These are interpreted as unconfined fluvial fan deposits in a position downstream from the amalgamated sands in the L2-8 area.

Besides the gradual north-to-south thinning and back-stepping pattern of the stratigraphic units in the entire basin (Fig. 2) there is a similar thinning and onlap pattern in an east-to-west direction

(Figs. 10–12). A broad south-to-north fluvial valley is thought to have existed in the erosive surface at the base of the URG (colloquially referred to as the Base Permian Unconformity, BPU), which gradually filled with the sediments of the URG (Neptune Energy Netherlands B.V. unpublished information; Geluk, 2007). Mapping the sand content of the lowstand packages also reveals a pattern of north-to-south back-stepping and a simultaneous east-to-west expansion through time, as is illustrated by the example of three of these units in Fig. 12. The sandy interval associated with, i.e. below, FS30 is limited to the deeper parts of the basin, whereas the one associated with FS110 extends to the west and that of FS140 is restricted to the south. As expected, the oldest deposits occur in the axial area of the valley, and over the course of time the valley filled up and the flanks were onlapped with sediments.

5. Discussion and conclusions

Long-range chronostratigraphic correlation in the central part of the Southern Permian Basin (SPB) in the Dutch offshore showed that the mud-prone Rotliegend succession contains thin-bedded and laterally very extensive sandstone packages with correlation lengths up to and over 100 km. The correlation technique of pattern matching of GR logs was strongly supported by calculating spectral trend curves (INPEFA).

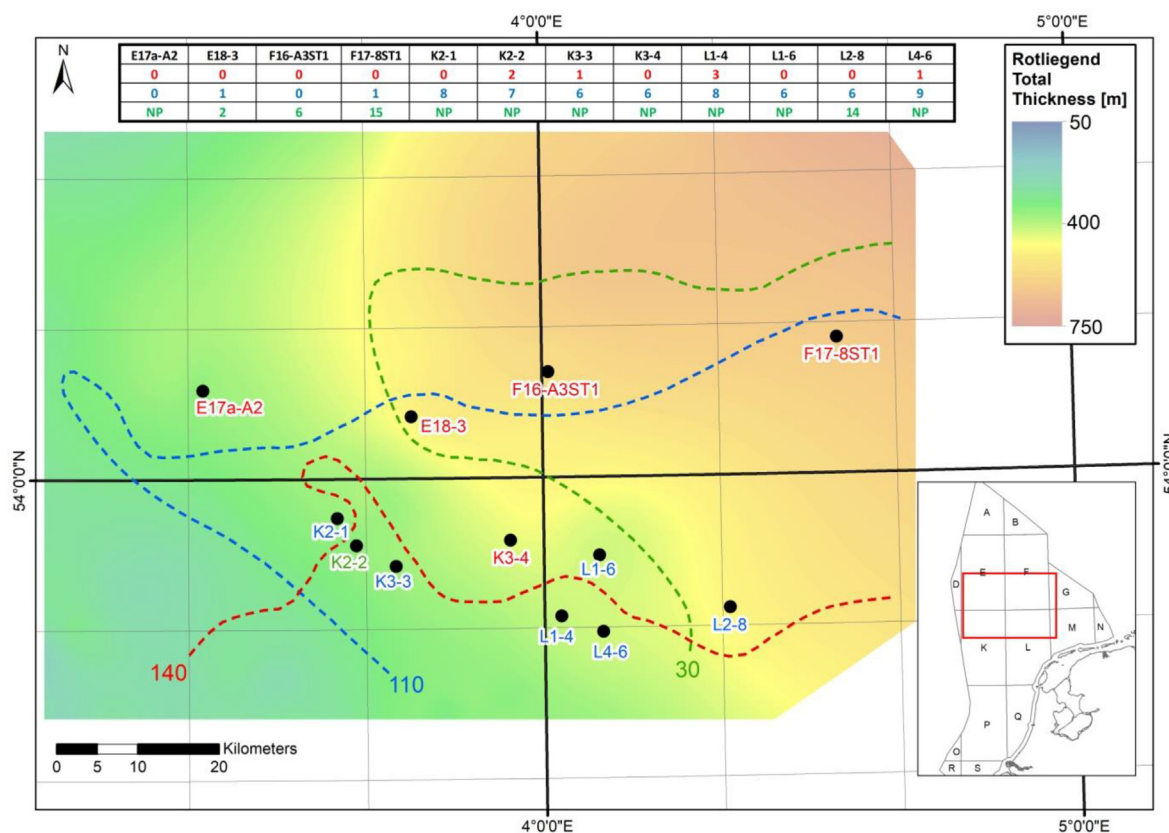


Fig. 12. Approximate distal boundary (dashed lines) of the sandy facies of the lowstand packages associated with (below) FS30 (green), FS110 (blue) and FS140 (red), overlying the generalized well-based isochore map of the total Rotliegend interval (excerpt from a larger map). Net sand thicknesses (m) are listed in the table (NP = not present). Note that sands with thicknesses below the resolution of the wireline logs are likely to occur beyond the distal boundaries. All wells in the map area have been used in the determination of the limits; only the location of the wells of Figs. 3–5, 10, 11 are displayed. (For interpretation of the references to colour in this figure legend, the reader is referred to the Web version of this article.)

Abrupt coarser-grained to finer-grained lithofacies changes in the succession have a characteristic C-shape expression in the GR and corresponding INPEFA curves, and the changes were interpreted as correlatable flooding surfaces. The surfaces are regional to supra-regional in extent and linked to events on the scale of the basin. In view of the large number of correlatable surfaces in the Rotliegend succession, the absence of internal unconformities, and the layer-cake stratigraphic architecture, it is proposed that the surfaces formed in response to climate change – probably as a function of Milankovitch periodicities – rather than as consequence of tectonics (Berger and Loutre, 1994; Gast et al., 2010; Perlmutter and Matthews, 1990; Perlmutter et al., 1998; Roscher and Schneider, 2006; Schröder et al., 1995). Using the analogue of well documented, climate-driven, late Quaternary lake-level fluctuations in the endorheic Altiplano Basin, we argue that similar fluctuations controlled the fluvial base-level in the endorheic SPB. The stratigraphic subdivision of the Upper Rotliegend of the adjacent German offshore is based on essentially the same principles (Schröder et al., 1995). Mechanisms of groundwater-table fluctuations in combination with expansion and contraction of desert lakes (George and Berry, 1994, 1997), or advancing and retreating desert fluvial systems (Fryberger et al., 2011) have been proposed as explanation for the stratigraphic cyclicity. The patterns presented here are better explained by larger-scale processes: large lake-level fluctuations, which may be considered an underestimated factor in understanding the Upper Rotliegend stratigraphy.

McKie (2011) discusses the relationship of depositional fabric in core and outcrop in the Rotliegend with modern dryland depositional processes and argues for prudence, stating that “uniformitarian principles are not universally applicable.” A similar topic is discussed by

Schröder et al. (1995) who state that identification of claystones formed during lake-level highstands in cored barren red-bed deposits is very difficult, if not impossible. Sediment supply to the basin centre during highstands is likely to be low, notably during short-lasting events, and highstand deposits may have been eroded or scoured during lake-level falls and lowstands, especially at the basin margin. A more fundamental issue is the integration of core and log data. This is often not straightforward – the Rotliegend red-beds are no exception – owing to the fact that each data type describes the different properties and dimensions (resolutions) of the rock bodies (Schröder et al., 1995).

The endorheic basin setting of the SPB, and the studied sandstone depositional architecture and sedimentary characteristics are analogous to the depositional setting of laterally-amalgamated terminal lobes of dryland-river systems in an endorheic basin during lowstands, such as the Holocene Altiplano Basin in Bolivia, present-day Lake Eyre (Australia) and the Miocene Ebro Basin (Spain). The terminal-lobe sandstones formed by successive upstream river avulsions which are triggered by the vertical aggradation of alluvial ridges and inherent decrease of the along-river gradient, thereby creating an intricate network of laterally-connected and amalgamated sandstone units. Unique for the endorheic basin setting is that a change from a drier to wetter climate period is translated in short-duration, high-magnitude base-level rise which is preserved in the rock record as basin-wide lacustrine mudstone draping the terminal lobes of the previous dry climate period. The model of Rotliegend basin fill in the central Dutch offshore allows predictions of the occurrence and volumetrics of potential sandstone reservoirs. More specifically, thin - i.e. below the vertical resolution of wireline logs – relatively coarse-grained terminal lobe deposits are located downstream from and connected with well-developed sandy

lowstand deposits, thus potentially adding to the gross rock volume of hydrocarbon reservoirs (Van Toorenburg et al., 2016).

CRedit authorship contribution statement

M.G.G. De Jong: Conceptualization, Methodology, Investigation, Formal analysis, Writing - original draft. **M.E. Donselaar:** Conceptualization, Methodology, Investigation, Writing - review & editing. **H.T.W. Boerboom:** Investigation. **K.A. Van Toorenburg:** Investigation. **G.J. Weltje:** Writing - review & editing. **L. Van Borren:** Project administration.

Declaration of competing interest

The authors declare that they have no known competing financial interests or personal relationships that could have appeared to influence the work reported in this paper.

Acknowledgements

Colleagues at Neptune Energy Netherlands B.V. are thanked for their contributions. The paper benefited from constructive comments of the reviewers. The study was carried out in conjunction with the TU Delft project Characterisation of Thin-bedded Gas Reservoirs, with financial support of Neptune Energy Netherlands B.V. and EBN B.V. (TU Delft project code C26B43).

Appendix A. Supplementary data

Supplementary data to this article can be found online at <https://doi.org/10.1016/j.marpetgeo.2020.104482>.

References

- Argollo, J., Mourguiart, P., 2000. Late quaternary climate history of the Bolivian Altiplano. *Quat. Int.* 72, 37–51.
- Baker, P.A., Rigsby, C.A., Seltzer, G.O., Fritz, S.C., Lowenstein, T.K., Bacher, N.P., Veliz, C., 2001. Tropical climate changes at millennial and orbital timescales on the Bolivian Altiplano. *Nature* 409, 698–701.
- Berger, A., Loutre, M.F., 1994. Astronomical forcing through geological time. In: De Boer, P.L., Smith, D.G. (Eds.), *Orbital Forcing and Cyclic Sequences*. vol. 19. International Association of Sedimentologists Spec. Publ., pp. 15–24.
- Bills, B.G., de Silva, S.L., Currey, D.R., Emenger, R.S., Lillquist, K.D., Donnellan, A., Worden, B., 1994. Hydro-isostatic deflection and tectonic tilting in the central Andes: initial results of a GPS survey of Lake Minchin shorelines. *Geophys. Res. Lett.* 21, 293–296.
- Blodgett, T., Lenters, J., Isaacs, B., 1997. Constraints on the origin of paleolake expansions in the central Andes. *Earth Interact.* 1, 1–28.
- Catuneanu, O., Abreu, V., Bhattacharya, J.P., Blum, M.D., Dalrymple, R.W., Eriksson, P.G., Fielding, C.R., Fisher, W.L., Galloway, W.E., Gibling, M.R., Giles, K.A., Holbrook, J.M., Jordan, R., Kendall, C.G.St.C., Macurda, B., Martinsen, O.J., Miall, A.D., Neal, J.E., Nummedal, D., Pomar, L., Posamentier, H.W., Pratt, B.R., Sarg, J.F., Shanley, K.W., Steel, R.J., Strasser, A., Tucker, M.E., Winker, C., 2009. Towards the standardization of sequence stratigraphy. *Earth Sci. Rev.* 92, 1–33.
- Dalman, R., Weltje, G.J., Karamitopoulos, P., 2015. High-resolution sequence stratigraphy of fluvio-deltaic systems: prospects of system-wide chronostratigraphic correlation. *Earth Planet Sci. Lett.* 412, 10–17.
- De Jager, J., 2007. Geological development. In: Batjes, D.A.J., De Jager, J. (Eds.), *Geology of the Netherlands*, Wong, Th. Royal Netherlands Academy of Arts and Sciences, pp. 5–26.
- De Jong, M.G.G., Donselaar, M.E., Boerboom, H.T.W., van Toorenburg, K.A., Weltje, G.J., van Borren, L., 2017. High-resolution reservoir architecture modelling of thin-bedded terminal-splay sandstone in the Rotliegend feather-edge area. In: *Proceedings 79th EAGE Conference & Exhibition, Paris, France, 12–15 June 2017*, Volume 1 of 7, pp. 397–401.
- De Jong, M.G.G., Nio, S.D., Böhm, A.R., Seijmonsbergen, A.C., de Graaff, L.W.S., 2009. Resolving climate change in the period 15–23 ka in Greenland ice cores: a new application of spectral trend analysis. *Terra. Nova* 21, 137–143.
- De Jong, M.G.G., Nio, S.D., Smith, D.G., Böhm, A.R., 2007. Subsurface correlation in the upper carboniferous (Westphalian) of the Anglo-Dutch basin using the climate stratigraphic approach. *First Break* 25, 49–59 December 2007.
- De Jong, M.G.G., Seijmonsbergen, A.C., de Graaff, L.W.S., 2019. In search of stratigraphic subdivision of the period 0–8 ka in Greenland ice cores. *Pol. Polar Res.* 40 (2), 55–77.
- De Jong, M., Smith, D., Nio, S.D., Hardy, N., 2006. Subsurface correlation of the Triassic of the UK southern Central Graben: new look at an old problem. *First Break* 24, 103–109 June 2006.
- Donselaar, M.E., Cuevas Gozalo, M.C., Moyano, S., 2013. Avulsion processes at the terminus of low-gradient semi-arid fluvial systems: lessons from the Río Colorado, Altiplano endorheic basin, Bolivia. *Sediment. Geol.* 283, 1–14.
- Donselaar, M.E., Cuevas Gozalo, M.C., Wallinga, J., 2017. Avulsion history of a holocene semi-arid river system: outcrop analogue for thin-bedded fluvial reservoirs in the rotliegend feather edge. In: *Proceedings 79th EAGE Conference & Exhibition, Paris, France, 12–15 June 2017*. Paper Th C1 05, 5 pp, <https://doi.org/10.3997/2214-4609.201700610>.
- Donselaar, M.E., Overeem, I., Reichwein, J.H.C., Visser, C.A., 2011. Mapping of fluvial fairways in the ten boer member, southern Permian Basin. In: Grötsch, J., Gaupp, R. (Eds.), *The Permian Rotliegend of The Netherlands*. SEPM Special Publication 98, 105–118.
- Doornenbal, J.C., Stevenson, A.G. (Eds.), 2010. *Petroleum Geological Atlas of the Southern Permian Basin Area*. Publications European Association of Geoscientists and Engineers, Houten.
- Fisher, J.A., Krapf, C.B.E., Lang, S.C., Nichols, G.J., Payenberg, T.H.D., 2008. Sedimentology and architecture of the Douglas Creek terminal splay, Lake Eyre, central Australia. *Sedimentology* 55, 1915–1930.
- Fisher, J.A., Nichols, G.J., Waltham, D.A., 2007. Unconfined flow deposits in distal sectors of fluvial distributary systems: examples from the Miocene Luna and Huesca Systems, northern Spain. *Sediment. Geol.* 195, 55–73. <https://doi.org/10.1016/j.sedgeo.2006.07.005>.
- Fornari, M., Risacher, F., Féraud, G., 2001. Dating of paleolakes in the central Altiplano of Bolivia. *Palaeogeogr. Palaeoclimatol. Palaeoecol.* 172, 269–282.
- Fryberger, S.G., Knight, R., Hern, C., Moscardiello, A., Kabel, S., 2011. Rotliegend facies, sedimentary provinces, and stratigraphy, Southern Permian Basin UK and The Netherlands. In: Grötsch, J., Gaupp, R. (Eds.), *The Permian Rotliegend of the Netherlands*. SEPM Special Publication 98, 51–88.
- Galloway, W.E., 1989. Genetic stratigraphic sequences in basin analysis I: architecture and genesis of flooding-surface bounded depositional units. *AAPG (Am. Assoc. Pet. Geol.) Bull.* 73 (2), 125–142.
- Gast, R.E., Duser, M., Breikreuz, C., Gaupp, R., Schneider, J.W., Stemmerik, L., Geluk, M.C., Geissler, M., Kiersnowski, H., Glennie, K.W., Kabel, S., Jones, N.S., 2010. Rotliegend. In: Doornenbal, J.C., Stevenson, A.G. (Eds.), *Petroleum Geological Atlas of the Southern Permian Basin Area*. EAGE Publications b.v., Houten, pp. 101–121.
- Geluk, M.C., 2005. *Stratigraphy and Tectonics of Permo-Triassic Basins in the Netherlands and Surrounding Areas*. PhD thesis. Utrecht University.
- Geluk, M.C., 2007. Permian. In: Batjes, D.A.J., De Jager, J. (Eds.), *Geology of the Netherlands*, Wong, Th. Royal Netherlands Academy of Arts and Sciences, pp. 63–83.
- George, G.T., Berry, J.K., 1994. A new palaeogeographic and depositional model of the upper Rotliegend, offshore The Netherlands. *First Break* 12 (3), 147–158.
- George, G.T., Berry, J.K., 1997. Permian (Upper Rotliegend) synsedimentary tectonics, basin development and palaeogeography of the southern North Sea. In: Ziegler, K., Turner, P., Daines, S.R. (Eds.), *Petroleum Geology of the Southern North Sea: Future Potential*. Geological Society, London, Special Publications 123, 31–61.
- Glennie, K.W., 1998. Lower Permian-Rotliegend. In: Glennie, K.W. (Ed.), *Petroleum Geology of the North Sea*. Blackwell Science Ltd, Oxford, pp. 137–173.
- Glennie, K.W., Provan, D.M.J., 1990. Lower permian Rotliegend reservoir of the southern North Sea gas province. In: Brooks, J. (Ed.), *Classic Petroleum Provinces*. Geological Society, London, Special Publications 50, 399–416.
- Grötsch, J., Gaupp, R. (Eds.), 2011. *The Permian Rotliegend of The Netherlands*. SEPM Special Publication, 98, Tulsa, Oklahoma.
- Howell, J., Mountney, N., 1997. Climatic cyclicity and accommodation space in arid to semi-arid depositional systems: an example from the Rotliegend Group of the UK southern North Sea. In: Ziegler, K., Turner, P., Daines, S.R. (Eds.), *Petroleum Geology of the Southern North Sea: Future Potential*. Geological Society Special Publication 123, 63–86.
- Henaes, S., Bloemsa, M.R., Donselaar, M.E., Mijnlief, H.F., Redjosefonto, A.E., Veldkamp, H.G., Weltje, G.J., 2014. The role of detrital anhydrite in diagenesis of aeolian sandstones (Upper Rotliegend, The Netherlands): implications for reservoir-quality prediction. *Sediment. Geol.* 314, 60–74.
- Kessler, A., 1984. The paleohydrology of the Late Pleistocene Lake Tauca on the southern Altiplano (Bolivia) and recent climatic fluctuations. In: Vogel, J.C. (Ed.), *Late Cainozoic Palaeoclimates of the Southern Hemisphere*, Proceedings of an international symposium held by the South African Society for Quaternary Research, Swaziland, 29 Aug.–2 Sep. 1983. Balkema, Rotterdam, 115–122.
- Legler, B., Schneider, J.W., 2008. Marine incursions into the Middle/Late Permian saline lake of the Southern Permian Basin (Rotliegend, Northern Germany) possibly linked to sea-level highstands in the Arctic rift system. *Palaeogeogr. Palaeoclimatol. Palaeoecol.* 26, 102–114.
- Martin, J.H., Evans, P.F., 1988. Reservoir modelling of aeolian/sabkha sequences, Southern North Sea (U.K. Sector). *Soc. Petrol. Eng. SPE* 18155, 473–486.
- Maynard, J.R., Gibson, J.P., 2001. Potential for subtle traps in the permian Rotliegend of the UK southern North Sea. *Petrol. Geosci.* 7, 301–314.
- McKie, T., 2011. A comparison of modern dryland depositional systems with the Rotliegend Group in The Netherlands. In: Grötsch, J., Gaupp, R. (Eds.), *The Permian Rotliegend of The Netherlands*. SEPM Special Publication 98, 89–103.
- Mijnlief, H.F., van Ojik, K., Nortier, J., Okkerman, J.A., Gaupp, R., Grötsch, J., 2011. The permian Rotliegend of The Netherlands: core atlas, appendix B. In: Grötsch, J., Gaupp, R. (Eds.), *The Permian Rotliegend of The Netherlands*. SEPM Special Publication 98, 281–371.
- Minervini, M., Rossi, M., Mellere, D., 2011. Cyclicity and facies relationships at the interaction between aeolian, fluvial, and playa depositional environments in the Upper Rotliegend: regional correlation across UK (Sole Pit Basin), The Netherlands, and Germany. In: Grötsch, J., Gaupp, R. (Eds.), *The Permian Rotliegend of The*

- Netherlands. SEPM Special Publication 98, 119-146.
- Moscariello, A., 2005. Exploration potential of the mature Southern North Sea basin margins: some unconventional plays based on alluvial and fluvial fan sedimentation models. In: Doré, A.G., Vining, B.A. (Eds.), *Petroleum Geology: North-West Europe and Global Perspectives*, Proceedings of the 6th Petroleum Geology Conference, 595-605.
- Moscariello, A., 2017. Alluvial fans and fluvial fans at the margins of continental sedimentary basins: geomorphic and sedimentological distinction for geo-energy exploration and development. In: Ventra, D., Clarke, L.E. (Eds.), *Geology and Geomorphology of Alluvial and Fluvial Fans: Terrestrial and Planetary Perspectives*. Geological Society, London, Special Publications 440, 215-243.
- Nio, S.D., Böhm, A.R., Brouwer, J.H., Jong, M.G.G. De, Smith, D.G., 2006. *Climate Stratigraphy, Principles and Applications in Subsurface Correlation*. EAGE Short Course Series. EAGE Publications b.v., Houten.
- Perlmutter, M.A., Matthews, M.D., 1990. Global cyclostratigraphy – a model. In: Cross, T. (Ed.), *Quantitative Dynamic Stratigraphy*. Prentice Hall, pp. 233-260.
- Perlmutter, M.A., Radovich, B.J., Matthews, M.D., Kendall, C.G.St.C., 1998. The impact of high frequency sedimentation cycles on stratigraphic interpretation. In: Gradstein, F., Sandvik, K.O., Milton, N.J. (Eds.), *Sequence Stratigraphy, Concepts and Applications*. Elsevier, pp. 141-170.
- Placzek, C., Quade, J., Patchett, P.J., 2006. Geochronology and stratigraphy of late Pleistocene lake cycles on the southern Bolivian Altiplano: implications for causes of tropical climate change. *Geol. Soc. Am. Bull.* 118, 515-532.
- Qayyum, F., Smith, D., 2014. Integrated sequence stratigraphy using trend logs and densely mapped seismic data. *First Break* 32, 75-84 December 2014.
- Reijers, T.J.A., Mijnlief, H.F., Pestman, P.J., Kouwe, W.F.P., 1993. Lithofacies and their interpretation: a guide to standardised description of sedimentary deposits. *Rijks Geol. Dienst* 49.
- Roscher, M., Schneider, J.W., 2006. Permo-Carboniferous climate: early Pennsylvanian to Late Permian climate development of central Europe in a regional and global context. *Geol. Soc. Lond. Spec. Publ.* 265, 95-136.
- Sáez, A., Anadón, P., Herrero, M.J., Moscariello, A., 2007. Variable style of transition between Paleogene fluvial fan and lacustrine systems, Southern Pyrenean foreland, NE Spain. *Sedimentology* 54, 367-390.
- Schröder, L., Plein, E., Bachmann, G.H., Gast, R.E., Gebhardt, U., Graf, R., Helmuth, H.-J., Pasternak, M., Porth, H., Süsmuth, S., 1995. Stratigraphische Neugliederung des Rotliegend im Norddeutschen Becken. *Geol. Jahrbuch* 148, 3-21.
- Sylvestre, F., Servant-Vildary, S., Fournier, M., Servant, M., 1996. Lake-levels in the southern Bolivian Altiplano (19°-21°S) during the Late Glacial based on diatom studies. *Int. J. Salt Lake Res.* 4, 281-300.
- Sylvestre, F., Servant, M., Servant-Vildary, S., Causse, C., Fournier, M., Ybert, J.-P., 1999. Lake-level chronology on the southern Bolivian Altiplano (18° - 23°S) during late glacial time and the early Holocene. *Quat. Res.* 51, 54-66.
- Van Adrichem Boogaert, H.A., 1976. Outline of the Rotliegend (lower permian) in The Netherlands. In: Falke, H. (Ed.), *The Continental Permian in Central, West, and South Europe*. D. Reidel Publishing Company, Dordrecht-Holland, pp. 23-37.
- Van Adrichem Boogaert, H.A., Kouwe, W.F.P., 1993. *Stratigraphic nomenclature of The Netherlands, revision and update by RGD and NOGEP*. Meded. Rijks Geol. Dienst 50.
- Van den Belt, F.J.G., Van Hulten, F.F.N., 2011. Sedimentary architecture and palaeogeography of Lower Slochteren aeolian cycles from the Rotliegend desert-lake margin (Permian), the Markham area, southern North Sea. In: Grötsch, J., Gaupp, R. (Eds.), *The Permian Rotliegend of The Netherlands*. SEPM Special Publication 98, 161-176.
- Van Ojik, K., Böhm, A., Cremer, H., Geluk, M.C., De Jong, M.G.G., Mijnlief, H.F., Nio, S.D., 2011. The rationale for an integrated stratigraphic framework of the Upper Rotliegend II depositional system in The Netherlands. In: Grötsch, J., Gaupp, R. (Eds.), *The Permian Rotliegend O The Netherlands*. SEPM Special Publication 98, 37-48.
- Van Toorenburg, K.A., 2018. *The Key Role of Crevasse Splays in Prograding River Systems - Analysis of Evolving Floodplain Accommodation and its Implications for Architecture and Reservoir Potential*. Published Doctorate thesis. Delft University of Technology, Delft, The Netherlands, 978-94-6366-084-6pp. 122.
- Van Toorenburg, K.A., Donselaar, M.E., Noordijk, N.A., Weltje, G.J., 2016. On the origin of crevasse-splay amalgamation in the Huesca fluvial fan (Ebro Basin, Spain): implications for connectivity in low net-to-gross fluvial deposits. *Sediment. Geol.* 343, 156-164.
- Van Toorenburg, K.A., Donselaar, M.E., Weltje, G.J., 2018. The life cycle of crevasse splays as a key mechanism in aggrading dryland rivers. *Earth Surf. Process. Landforms* 43, 2409-2420. <https://doi.org/10.1002/esp.4404>.
- Van Wees, J.-D., Stephenson, R.A., Ziegler, P.A., Bayer, U., McCann, T., Dadlez, R., Gaupp, R., Narkiewicz, M., Bitzer, F., Scheck, M., 2000. On the origin of the southern Permian Basin, central Europe. *Mar. Petrol. Geol.* 17, 43-59.
- Verdier, J.P., 1996. The Rotliegend sedimentation history of the southern North Sea and adjacent countries. In: Rondeel, H.E., Batjes, D.A.J., Nieuwenhuijs, W.H. (Eds.), *Geology of Gas and Oil under the Netherlands*. Kluwer Academic Publishers, Dordrecht, pp. 45-56.